Two-photon resonant, optical third-harmonic generation in cesium vapor*

K. M. Leung† and J. F. Ward
The Harrison M. Randall Laboratory of Physics, University of Michigan, Ann Arbor, Michigan 48104

B. J. Orr
Department of Physical Chemistry, University of New South Wales, New South Wales 2033, Australia

(Received 28 January 1974)

Resonant enhancement of optical third-harmonic generation in cesium vapor has been observed when twice the energy of the fundamental photon becomes equal to the energy difference between the $9d\ ^2D_{3/2}$ level and the ground state of the cesium atom. The measured, effective coefficient is 10^{-30} esu/atom, which is more than a factor 10^8 larger than the corresponding coefficient for the helium atom. An effective coefficient is synthesized by first calculating the coefficient for a single cesium atom at rest and then including the effects of Doppler broadening and the fundamental laser spectrum. The calculated value is in satisfactory agreement with experiment.

I. INTRODUCTION

We wish to report the observation of resonant optical third-harmonic generation in cesium vapor.[1] The resonance investigated here occurs when twice the fundamental photon energy ($2hc\omega$) becomes equal to the energy difference between the $9d\ ^2D_{3/2}$ level and the ground state for a cesium atom.

This resonance is conveniently discussed in terms of a time-dependent perturbation-theoretic expression for the third-harmonic coefficient $\chi(-3\omega;\omega,\omega,\omega)$. A generalized definition of such coefficients is given by the relation between Fourier amplitudes of the applied electric fields $\vec{E}^{\omega_1}$, $\vec{E}^{\omega_2},\ldots$, and the resulting dipole moment $\vec{p}^{\omega_\sigma}$:

$$\vec{p}^{\omega_\sigma} = K(-\omega_\sigma;\omega_1,\omega_2,\ldots)\,\chi(-\omega_\sigma;\omega_1,\omega_2,\ldots) \times \vec{E}^{\omega_1}\vec{E}^{\omega_2}\ldots, \tag{1}$$

where frequencies are indicated by superscripts and satisfy

$$\omega_\sigma = \omega_1 + \omega_2 \ldots \tag{2}$$

and $\chi(-\omega_\sigma;\omega_1,\omega_2,\ldots)$ is the (tensor) coefficient for the process. $K(-\omega_\sigma;\omega_1,\omega_2,\ldots)$ is a number of order unity and is discussed in Refs. 2 and 3, together with other details of the conventions used here. Time-dependent perturbation-theoretic expressions for $\chi(-\omega_\sigma;\omega_1,\omega_2,\ldots)$ are available in the literature[2] and typical terms for polarizations linear, second order, and third order in the applied electric field may be written

Linear

$$\chi(-\omega_1;\omega_1) \propto \frac{\langle g|r|n\rangle\langle n|r|g\rangle}{\Omega_{ng}-\omega_1} + \ldots, \tag{3}$$

Second order

$$\chi(-\omega_\sigma;\omega_1,\omega_2) \propto \frac{\langle g|r|l\rangle\langle l|r|n\rangle\langle n|r|g\rangle}{(\Omega_{lg}-\omega_1-\omega_2)(\Omega_{ng}-\omega_1)} + \ldots, \tag{4}$$

Third order

$$\chi(-\omega_\sigma;\omega_1,\omega_2,\omega_3) \propto \frac{\langle g|r|l\rangle\langle l|r|m\rangle\langle m|r|n\rangle\langle n|r|g\rangle}{(\Omega_{lg}-\omega_1-\omega_2-\omega_3)(\Omega_{mg}-\omega_1-\omega_2)(\Omega_{ng}-\omega_1)} + \ldots, \tag{5}$$

where $|g\rangle$ is the ground state, $|m\rangle$ denotes an intermediate state with energy $hc\omega_m$, and lifetime Γ_m^{-1}, and

$$\Omega_{mg} = (\omega_m - \omega_g) - i\tfrac{1}{2}\Gamma_m . \tag{6}$$

A resonance occurs whenever an applied field frequency is such that the real part of a resonance denominator vanishes. For example,

$$\begin{aligned} &\mathrm{Re}(\Omega_{ng}-\omega_1)=0,\\ &\mathrm{Re}(\Omega_{mg}-\omega_1-\omega_2)=0,\\ &\mathrm{Re}(\Omega_{lg}-\omega_1-\omega_2-\omega_3)=0, \end{aligned} \tag{7}$$

which are representative of one-, two-, and three-photon resonances, respectively. The familiar one-photon resonances in the linear polarizability give rise to absorption and a region of "anomalous" dispersion. Second- and third-order coefficients become large and complex near a resonance, but such resonances are usually accompanied by linear resonance (and therefore absorption) at either an applied field or polarization frequency. This situation has been analyzed by a number of authors.[4] In the case of the two-photon resonance in the third-order coefficient,

$$\mathrm{Re}(\Omega_{mg} - \omega_1 - \omega_2) = 0\,, \tag{8}$$

a new feature arises which is absent in lower-order processes. Resonant enhancement of the coefficient can occur *without* linear absorption at any field or polarization frequency. This type of resonance is involved in the stimulated Raman effect and subsequent four-wave interactions.[5] *Nonlinear* (two-photon) absorption processes arising, for example, from $\mathrm{Im}[\chi(-\omega_2;\ \omega_2,\ -\omega_1,\ \omega_1)]$ do accompany the other two-photon resonant third-order processes, but these are much weaker than linear absorption. Two-photon absorption has been studied in various materials,[6] including measurements by Abella in cesium vapor.[7]

The resonant third-harmonic generation studied here arises from a two-photon resonance and in this particular case Eq. (5) becomes

$$\chi(-3\omega;\ \omega,\ \omega,\ \omega) \propto \frac{\langle g|r|l\rangle\langle l|r|m\rangle\langle m|r|n\rangle\langle n|r|g\rangle}{(\Omega_{lg} - 3\omega)(\Omega_{mg} - 2\omega)(\Omega_{ng} - \omega)} + \cdots\,. \tag{9}$$

The condition for the resonance is

$$\mathrm{Re}(\Omega_{mg} - 2\omega) = 0\,, \tag{10}$$

and also the relevant matrix-element product must not vanish—

$$\langle m|r|n\rangle\langle n|r|g\rangle \neq 0\,; \tag{11}$$

thus if $|g\rangle$ is an atomic S state, $|m\rangle$ must be an S or D state. Both conditions can be met using a ruby-laser source and cesium vapor as the resonant third-harmonic generator. Figure 1 shows an energy-level diagram for cesium with the $9d\,^2D_{3/2}$ level accentuated. This level is 28818.90 cm^{-1} above the ground state, and the ruby-laser output can be tuned to half this value by cooling the ruby rod to about 148°K. We were not able to tune our ruby laser to achieve resonance with the $9d\,^2D_{5/2}$ level at 28836.06 cm^{-1}, and the nearest S level (11s) is much further away at 29130 cm^{-1}.

It may be noted from Fig. 1(a) that the third harmonic is beyond the ionization limit for cesium. This does not have a dramatic effect on either the third-harmonic coefficient or the linear absorption of the third harmonic.

In Fig. 1(b) the process observed by Abella[7] is indicated schematically. The solid lines indicate population of the $9d\,^2D_{3/2}$ level by two-photon absorption. This process clearly has the same resonant dependence on fundamental frequency as third-harmonic generation. Dashed lines indicate one of several fluorescent decay paths for the excited $9d\,^2D_{3/2}$ level.

Simultaneous observation of the fluorescence and third-harmonic generation which provides a definitive signature for this resonance will be described in Sec. II. In Sec. III we synthesize an effective third-harmonic coefficient for comparison with the measured value. This synthesis includes the effects of Doppler broadening and the laser spectrum, and is based on a quantum-mechanical calculation described in the Appendix for a single cesium atom at rest.

II. EXPERIMENTAL

A schematic diagram of the apparatus is shown in Fig. 2.

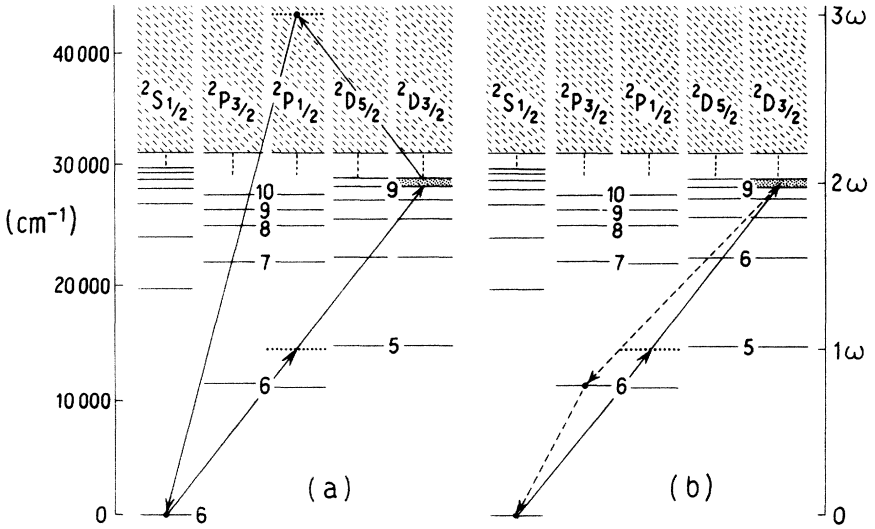

FIG. 1. Energy-level diagram for the cesium atom showing schematically (a) resonant third-harmonic generation and (b) two-photon absorption (solid lines) followed by two-step fluorescent decay (dashed lines). The resonant $9d\,^2D_{3/2}$ level is shown emphasized and ω is the frequency of the incident light.

The Q-switched ruby laser produces a 1-MW 25-nsec [full width at half-maximum (FWHM)] light pulse. The rod temperature is controlled in the range 293–125°K, which corresponds to an output wavelength range[8] of 694.3–693.5 nm. The laser output exhibits multi-transverse-mode structure: The longitudinal mode structure is discussed in Sec. III.

The cesium vapor is contained in an 18-cm-long stainless-steel cell with sapphire windows. Heating tapes and cooling coils maintain a temperature distribution along the cell, highest at the center, falling to a minimum at 6 cm from the center, and rising again at the windows. A typical temperature at the center of the cell is 483°K, which corresponds to a cesium-vapor pressure[9] of about 0.13 Torr. The cell is lined with copper felt, which serves as a wick to return liquid cesium to the center of the cell. About 1 Torr of neon was introduced into the cell before sealing off prior to the experiments. This buffer gas, together with the temperature distribution, inhibits diffusion of cesium vapor to the cell windows which, in the presence of the laser beam, would lead to incandescence and window damage. The neon has no other significant effect on the experiment. The cell is provided with a third window to permit observation of light emitted by the cesium vapor in a direction perpendicular to the laser beam.

Third-harmonic and fluorescent radiation are detected by photomultipliers after suitable spectral filtering (see Fig. 2). The two photomultiplier output pulses are shown sequentially on one beam of a dual-beam oscilloscope with the other beam displaying a fundamental intensity-monitor pulse. Photographs of these oscilloscope traces yield pulse heights proportional to fundamental power $\mathcal{P}^{\omega}$, third harmonic power $\mathcal{P}^{3\omega}$, and fluorescent signal power $\mathcal{P}^{f}$.

A third-harmonic signal exhibiting the expected pulse duration, wavelength, and polarization appeared as the cesium cell was heated up from room temperature. For these experiments the laser beam was focused at the center of the cesium cell and about 5 μW of harmonic was generated with the fundamental attenuated to 120 kW. The dependence of harmonic generation on fundamental frequency (ruby-rod temperature) was then investigated, with the cesium-cell temperature distribution maintained constant with the center at 483°K. The observed resonance is shown in Fig. 3(a). The error bars in Fig. 3 represent the statistical uncertainty over a set of 15 laser shots. The fundamental frequency scale was calibrated to within ± 0.05 cm^{-1} (as indicated in Fig. 3 by a horizontal error flag) with respect to standard cadmium lines using a grating spectrograph. The vertical arrow indicates the expected position of the resonance peak at $\frac{1}{2}\omega_{9D_{3/2}} = 14414.45$ cm^{-1} and the agreement with experiment is excellent. Also shown in Fig. 3(b) is the simultaneously observed fluorescent light emitted through the side window at 584.7 nm. This arises from the fluorescent decay to the $6p\,^2P_{3/2}$ level from the $9d\,^2D_{3/2}$ level populated by two-photon absorption, which was studied in detail by Abella.[7] We have also observed fluorescence at 566.6 nm from the transition $9d\,^2D_{3/2}$-$6p\,^2P_{1/2}$, which, as expected, is five times as intense as the 584.7-nm component. It can be seen that this resonant effect also occurs at the predicted fundamental wavelength and is coincident with the resonant third harmonic.

The linewidths of the two resonance curves are comparable, being 0.30 and 0.20 cm^{-1} (FWHM) for third harmonic and fluorescence, respectively. This feature and the line shape will be discussed further in Sec. III.

The effective atomic third-harmonic coefficient at the peak of the resonance was measured using a collimated fundamental beam. In this case it can be shown that the amount of harmonic generated depends only on the number of coherence

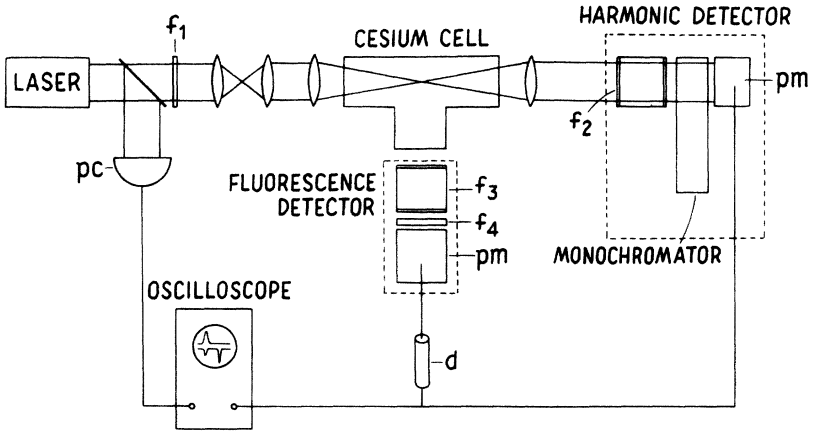

FIG. 2. Schematic diagram of the apparatus. d: delay line; f_1: red transmitting filter; f_2: aqueous $NiSO_4$ filter; f_3: aqueous $CuSO_4$ filter; f_4: interference filter 566.6 or 584.7 nm; pm: photomultiplier RCA 1P28; pc: photocell RCA 922.

lengths of cesium vapor traversed by the beam, and not on the cesium distribution. (Detailed consideration of harmonic generation by focused beams in inhomogeneous media will be presented elsewhere.) As the temperature at the center of the cesium cell is raised the observed harmonic signal increases to a maximum and then drops to zero again (see Fig. 4). The maximum can be identified with the presence of one coherence length of cesium vapor. [Calculations based on the cell exterior temperature distribution, vapor-pressure data, [9] and calculated optical polarizabilities (see Appendix), give the same result to within 20%.] The effective coefficient $\langle\chi\rangle$ may be obtained from the measured fundamental and harmonic powers measured at one coherence length, according to the relation

$$\frac{\mathcal{P}^{\omega}}{(\mathcal{P}^{\omega})^3} = 16\pi^2 \frac{|\langle\chi\rangle|^2}{c^2A^2[\alpha(\omega)-\alpha(3\omega)]^2}, \tag{12}$$

where A is the cross-sectional area of the fundamental beam. $\alpha(\omega)$ and $\alpha(3\omega)$ are the linear atomic polarizabilities at the fundamental and harmonic, respectively, for which we use calculated values (see Appendix).

The sensitivity of the apparatus was calibrated by observing third-harmonic generation in helium gas and using a theoretical value for the helium coefficient.[10] This yields

$$\langle\chi\rangle = 10^{-30} \text{ esu/atom} \tag{13}$$

with an estimated uncertainty of a factor of 5. $\langle\chi\rangle$ is an effective coefficient in the sense that it depends on the broadening processes taking place in the cesium vapor and on the laser spectrum, as well as on intrinsic properties of a cesium atom. This will be discussed in detail in Sec. III.

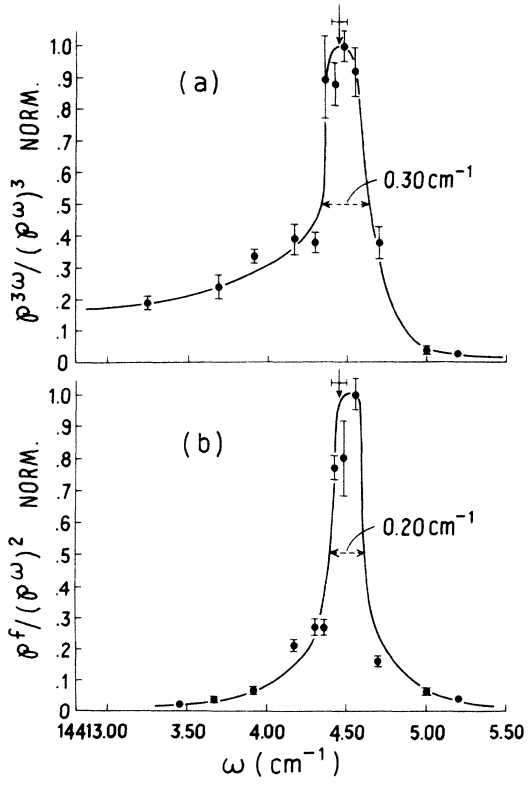

FIG. 3. Third-harmonic generation (a), and $9d\,^2D_{3/2}$-$6p\,^2P_{3/2}$ fluorescence following two-photon population of the $9d\,^2D_{3/2}$ level (b), as a function of fundamental light frequency. The vertical arrow indicates the expected position of the resonance with horizontal error flag showing the uncertainty in our frequency scale calibration. Vertical error flags indicate statistical uncertainty over 15 laser shots.

III. SYNTHESIS OF EFFECTIVE COEFFICIENT $\langle\chi\rangle$

In this section we present results of a quantum-mechanical calculation for the resonant third-order nonlinear coefficient of a single cesium atom at rest. (The calculation is outlined in the Appendix.) The effects of Doppler broadening and laser spectrum are then included to synthesize an effective coefficient for comparison with experiment.

Near the resonance

$$\mathrm{Re}(\Omega_{m\varepsilon} - \omega_1 - \omega_2) = 0 \tag{14}$$

the dominant resonant part of the nonlinear coefficient $\chi_{zzzz}(-\omega_\sigma; \omega_1, \omega_2, \omega_3)$ may be written[2]

$$\chi_{zzzz}(-\omega_\sigma; \omega_1, \omega_2, \omega_3) = \chi_0 I_{1,2,3}\left(\frac{\frac{1}{2}\Gamma_m}{\Omega_{m\varepsilon} - \omega_1 - \omega_2}\right), \tag{15}$$

where $I_{1,2,3}$ indicates the average of all terms obtained by permuting ω_1, ω_2, ω_3. For the cesium

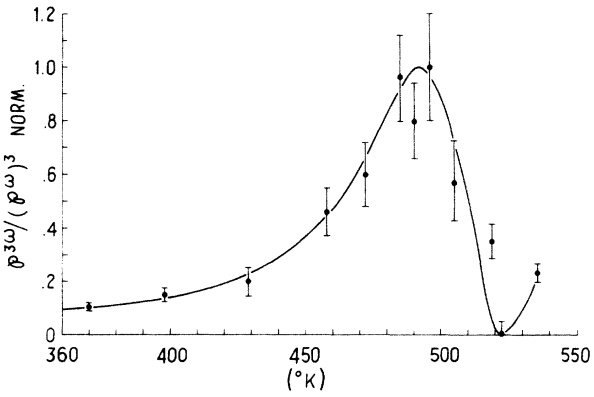

FIG. 4. Third-harmonic generation by a collimated fundamental beam, as a function of temperature at the center of the cesium cell. The maximum corresponds to the presence of one coherence length of cesium vapor. A smooth curve has been drawn to fit the data points.

atom and with m denoting the $9d\,^2D_{3/2}$ state we have

$$\Omega_{mg} = \omega_{mg} - i\tfrac{1}{2}\Gamma_m$$
$$= (28818.90 - \tfrac{1}{2}i \times 1.9 \times 10^{-5})\ \mathrm{cm}^{-1} \qquad (16)$$

and we find (as discussed in the Appendix)

$$\chi_0 = (8.8 \pm 4) \times 10^{-27}\ \mathrm{esu/atom}. \qquad (17)$$

It should be noted that, whereas a complex linear polarizability implies absorption, this is not the case for the third-harmonic coefficient. Real and imaginary parts of the nonlinear coefficient [which are illustrated in Fig. 5(a)] give rise to two harmonic components in phase quadrature which both contribute to the harmonic power $\mathcal{P}^{3\omega}$, so that $\mathcal{P}^{3\omega}$ is proportional to the square of the absolute value of the harmonic coefficient.

A. Doppler broadening

The experimental resonance curve is modified by Doppler broadening arising from thermal motion of the cesium atoms. The effect is essentially to broaden the resonance curve symmetrically from $\frac{1}{2}\Gamma_m$ (natural width) to Γ_D (Doppler width) and reduce the peak intensity by a factor close to $(\Gamma_m/\Gamma_D)^2$. For a more quantitative analysis we first note that the width γ (FWHM) of the distribution of a normalized velocity component, say, v_z/c, for cesium atoms of mass M at temperature $T = 483\,^\circ\mathrm{K}$ is given by

$$\gamma = \left(\frac{8kT\ln 2}{Mc^2}\right)^{1/2}$$
$$= 1.4 \times 10^{-6}. \qquad (18)$$

Using tabulated values of the plasma dispersion function[11] yields the Doppler-averaged atomic coefficient $\langle\chi\rangle_D$ as a function of laser frequency ω shown in Fig. 5(b). It is found that, at resonance,

$$|\langle\chi\rangle_D| = |\chi_0| \frac{\Gamma_m/\omega_{mg}}{\gamma} (\pi \ln 2)^{1/2}$$
$$= 6.3 \times 10^{-30}\ \mathrm{esu/atom} \qquad (19)$$

and the width Γ_D (FWHM) of the resonance curve due to Doppler broadening is

$$\Gamma_D = 0.024\ \mathrm{cm}^{-1}. \qquad (20)$$

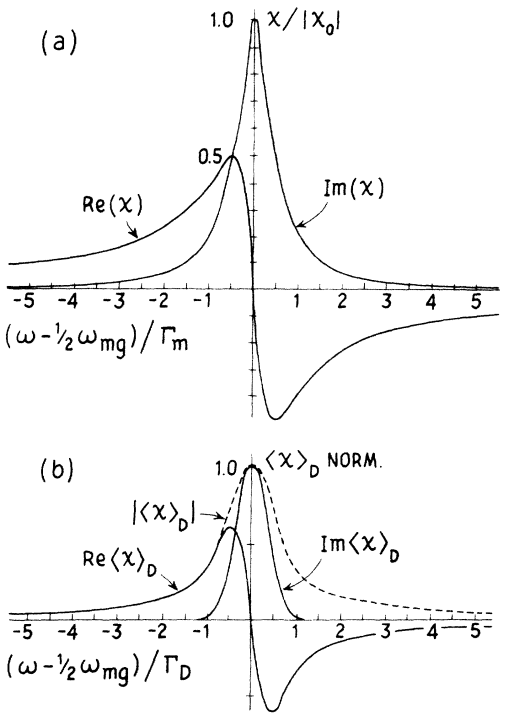

FIG. 5. Frequency dependence of resonant coefficients. (a) For an atom at rest; width determined by the natural width Γ_m. (b) Average coefficients for moving atoms; width determined by the Doppler effect.

B. Laser spectrum

Investigation of the laser spectrum using a 2.5-cm Fabry-Perot interferometer indicated the presence of several longitudinal modes. We now calculate the effect on the third-harmonic resonance curve for the following simplified mode structure, which approximates that experimentally observed: a number of mutually incoherent longitudinal modes of equal power and separated by $\epsilon = 0.025\ \mathrm{cm}^{-1}$, which corresponds to the optical length of the laser rod. Consider, for example, the case of three modes, with frequencies $\omega - \epsilon$, ω, and $\omega + \epsilon$ as ω is scanned through the resonance region. There are ten different ways to sum three frequencies from this list, which all give resultant frequencies in the range $3\omega - 3\epsilon$ to $3\omega + 3\epsilon$. This whole range is well within the detector bandwidth and all ten processes contribute to the observed "third-harmonic" signal.

One of the ten processes, for example, can be represented by

$$3\omega \leftarrow (\omega + \epsilon) + (\omega) + (\omega - \epsilon). \qquad (21)$$

K for this process [see Eq. (1)] is $\frac{3}{2}$ and there are three resonant terms to include in Eq. (15) at

$$\omega = \tfrac{1}{2}\omega_{mg} - \epsilon,\ \tfrac{1}{2}\omega_{mg},\ \tfrac{1}{2}\omega_{mg} + \epsilon. \qquad (22)$$

The frequency dependence of the coefficient for this process with Doppler broadening taken into account is easily constructed knowing the frequency dependence of $\langle\chi\rangle_D$. The single resonance in $\langle\chi\rangle_D$ [see Fig. 5(b)] is resolved into three similar resonances, two of them displaced in frequency

by $\pm\epsilon$, respectively, as required by Eq. (22).

The frequency-dependent coefficients for the other nine contributing processes are then constructed in an analogous fashion. The ten processes are mutually incoherent, as we have assumed the three fundamental modes to be mutually incoherent. Thus the absolute magnitude of the over-all effective coefficient at a particular frequency ω is the square root of the sum of the squares of the real and imaginary parts of the coefficient for each of the ten processes at frequency ω. The resulting computed resonance curve for three modes is shown in Fig. 6, along with results for one, five, and seven modes. It should be noted that the peak height is increased by going from a single mode to three modes. This is because the decrease due to broadening is more than compensated for by the increase due to the greater number of possible mixing processes. Moreover, the penalty for increasing the number of modes to five or seven is not severe. In fact, the number of modes in the laser output decreases from about seven to five as the laser frequency is varied from 14414 to 14415 cm^{-1} through the resonance. An appropriate interpolation to represent this experimental situation is shown as a dashed curve in Fig. 6. Therefore, taking Doppler broadening and our particular laser spectrum into account, we predict from Fig. 6 the effective coefficient

$$|\langle\chi\rangle| = 4.9\times10^{-30}\ \text{esu/atom} \tag{23}$$

and a corresponding width for the resonance Γ (FWHM),

$$\Gamma = 0.11\ cm^{-1}. \tag{24}$$

The predicted resonance curve is asymmetric due to the change in the number of modes as the laser center frequency is varied, but the asymmetry is slight for the simplified model of laser spectrum discussed here.

C. Comparison of experimental results with predicted values

The experimental resonance curve is substantially more asymmetric than the predicted curve. This may arise from features of the temperature-dependent mode structure not allowed for in our model.

The observed resonance curve is about three times as wide as predicted, and this is not, at present, understood. We have considered pressure-dependent broadening[12] due to Cs-Cs or Cs-Ne collisions, but estimate this to be insignificant. Moreover, peak harmonic signal is found to be essentially constant, as cesium vapor pressure is increased to give successively one, three, five, and seven coherence lengths of cesium in the cell, which implies that the resonance width is not significantly dependent on pressure.[13]

We estimate the effective coefficient in the presence of the unknown broadening mechanism by assuming that the area under the resonance curve remains unchanged. This yields finally

$$|\langle\chi\rangle|_{\text{pred}} = 3.0\times10^{-30}\ \text{esu/atom}, \tag{25}$$

which is to be compared with the experimental value

$$|\langle\chi\rangle|_{\text{expt}} = 10^{-30}\ \text{esu/atom}. \tag{26}$$

The estimated uncertainties are large (including

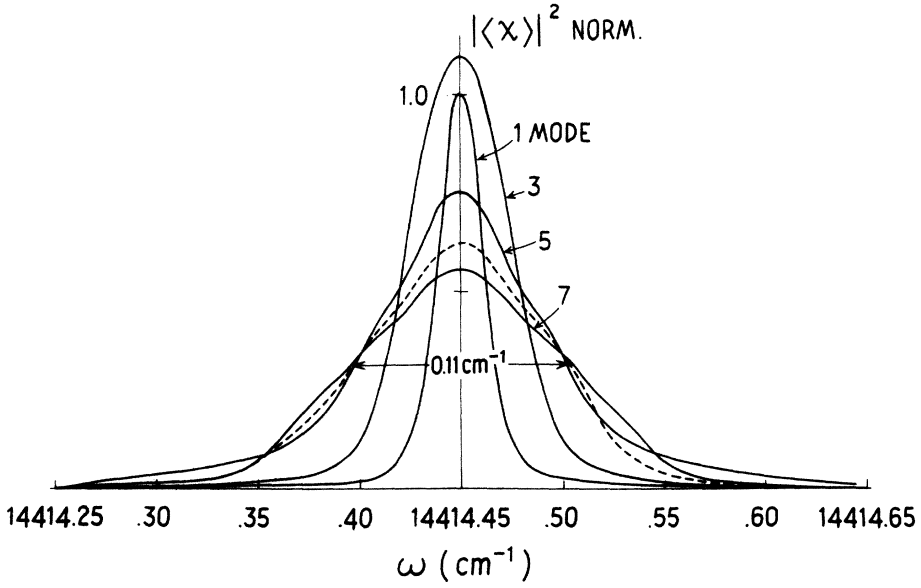

FIG. 6. Computed effect of laser spectrum on the effective resonant coefficient. Each curve is labeled 1, 3, 5, 7 to indicate the number of modes with equal power, and separated by 0.025 cm^{-1}, for which the curve was computed. The absolute value of the coefficient, squared and normalized to a peak value of unity for the single-mode case, is plotted against ω, the frequency of the center mode. The dashed curve represents an interpolation appropriate to the experimental laser whose spectrum varied with ω from seven to five modes in the resonance region.

±50% in the quantum-mechanical calculation and a factor of 5, in the experimental value), but we find the consistency between theory and experiment very satisfactory.

IV. CONCLUSIONS

We have demonstrated enhancement of optical third-harmonic generation in cesium vapor at a two-photon resonance.

The measured resonant coefficient is in satisfactory agreement with a value which we have calculated, starting from a quantum-mechanical calculation for a cesium atom at rest and taking into account Doppler broadening and the effect of the laser spectrum. The presence of several longitudinal modes in the fundamental laser beam does not severely reduce the amount of third harmonic generated.

The measured effective cesium coefficient is about 100 times larger than that measured for rubidium by Young *et al.*[14] and more than 10^8 times larger than the corresponding coefficient for helium.[3,10] It is clear that two-photon resonant enhancement will be an important feature in schemes for efficient frequency conversion using third-order nonlinearities.

ACKNOWLEDGMENT

It is a pleasure to acknowledge stimulating discussions with M. P. Bogaard and to thank him for assistance with computing.

APPENDIX: EVALUATION OF RESONANT NONLINEAR COEFFICIENTS

In this Appendix we outline the evaluation of the nonlinear optical coefficient χ_0 [Eq. (15)], describing third-harmonic generation for a cesium atom at rest in the vicinity of a $9d\,^2D \leftarrow 6s\,^2S$ two-photon resonance. Although only the $9d\,^2D_{3/2} \leftarrow 6s\,^2S_{1/2}$ resonance has been observable in the above experiments, it is useful to estimate also the coefficient for the adjacent $9d\,^2D_{5/2} \leftarrow 6s\,^2S_{1/2}$ resonance. The calculations involve term-by-term summation of perturbation-theory formulas; such an approach has been successfully applied to resonant atomic hyperpolarizabilities for sodium and lithium.[15]

The relevant nonlinear susceptibility[3] for a two-photon resonance $m \leftarrow g$ may be obtained by extracting resonant terms from Eq. (43c) of Ref. 2:

$$\chi_{zzzz}^{m\leftarrow g}(-\omega_\sigma;\omega_1,\omega_2,\omega_3)=\frac{e^4}{(hc)^3}I_{1,2,3}\left(\mathrm{S}_n'\frac{\langle m|z|n\rangle\langle n|z|g\rangle}{\omega_{ng}-\omega_1}\right)\{\mathrm{S}_l'\langle g|z|l\rangle\langle l|z|m\rangle[(\omega_{mg}-\omega_\sigma)^{-1}+(\omega_{lg}+\omega_3)^{-1}]\}$$
$$\times(\Omega_{mg}-\omega_1-\omega_2)^{-1}, \tag{A1}$$

where the notation $\omega_{ng}=\mathrm{Re}(\Omega_{ng})=\omega_n-\omega_g$ is used and S_n' denotes a summation over all discrete and continuous intermediate states n, excluding the ground state g. Radiative damping has been retained only in the resonant denominator $(\Omega_{mg}-\omega_1-\omega_2)$.

In the case of a cesium atom in the vicinity of the two $9d\,^2D_j \leftarrow 6s\,^2S_{1/2}$ resonances, where $j=\frac{3}{2}$ or $\frac{5}{2}$, Eq. (A1) reduces to

$$\chi_{zzzz}^{9D_{3/2}\leftarrow 6S_{1/2}}(\omega_\sigma;\omega_1,\omega_2,\omega_3)=\frac{e^4}{(hc)^3}I_{1,2,3}\frac{8}{5}(\Omega_{9D_{3/2}}-\omega_1-\omega_2)^{-1}\left[\frac{5}{6}\sum_n A_n\left(\frac{1}{2};\frac{3}{2}\right)+\frac{1}{6}\sum_n A_n\left(\frac{3}{2};\frac{3}{2}\right)+\int_0^\infty A(\epsilon')\,d\epsilon'\right]$$
$$\times\left[\frac{5}{6}\sum_{n'} B_{n'}\left(\frac{1}{2};\frac{3}{2}\right)+\frac{1}{6}\sum_{n'} B_{n'}\left(\frac{3}{2};\frac{3}{2}\right)+\int_0^\infty B(\epsilon')\,d\epsilon'\right], \tag{A2}$$

$$\chi_{zzzz}^{9D_{5/2}\leftarrow 6S_{1/2}}(-\omega_\sigma;\omega_1,\omega_2,\omega_3)=\frac{e^4}{(hc)^3}I_{1,2,3}\frac{12}{5}(\Omega_{9D_{5/2}}-\omega_1-\omega_2)^{-1}\left[\sum_n A_n\left(\frac{3}{2};\frac{5}{2}\right)+\int_0^\infty A(\epsilon')\,d\epsilon'\right]$$
$$\times\left[\sum_{n'} B_{n'}\left(\frac{3}{2};\frac{5}{2}\right)+\int_0^\infty B(\epsilon')\,d\epsilon'\right], \tag{A3}$$

where $\sum_n$ denotes a summation over the principal quantum number n for discrete intermediate states $|np^2P_{j'}\rangle$ and the integrals are over all values of the energy ϵ' of the ionized electron in a continuum p state, $|\epsilon' p\rangle$. The quantities A and B are defined by

$$A_n(j';j)=(\omega_{nP_{j'}}-\omega_1)^{-1}\sigma(9dj;npj')\sigma(npj';6s\tfrac{1}{2}), \tag{A4}$$

$$B_n(j',j)=[(\omega_{nP_{j'}}-\omega_\sigma)^{-1}+(\omega_{nP_{j'}}+\omega_3)^{-1}]$$
$$\times\sigma(6s\tfrac{1}{2};npj')\sigma(npj';9dj), \tag{A5}$$

$$A(\epsilon')=(I_{6S}+\epsilon'-\omega_1)^{-1}\sigma(9d;\epsilon' p)\sigma(\epsilon' p;6s), \tag{A6}$$

$$B(\epsilon')=[(I_{6S}+\epsilon'-\omega_\sigma)^{-1}+(I_{6S}+\epsilon'+\omega_3)^{-1}]$$
$$\times\sigma(6s;\epsilon' p)\sigma(\epsilon' p;9d), \tag{A7}$$

where $\omega_{nP_{j'}}$ is the frequency for the transition $np^2P_{j'} \leftarrow 6s\,^2S_{1/2}$ and I_{6S} is the ionization potential of cesium in its $6s\,^2S_{1/2}$ ground level. The reduced matrix elements $\sigma(n'\,l-1\,j';nlj)$ are related to the radial parts, $r^{-1}R_{nlj}$, of single-valence electron states $|nljm\rangle$ by

$$\sigma(n'\,l-1j';nlj)=(4l^2-1)^{-1/2}\int_0^\infty R_{n'\,l-1\,j'}R_{nlj}r\,dr\,. \tag{A8}$$

They are readily related to normal dipole-matrix elements $\langle n'\,l'\,j'\,m'|z|nljm\rangle$ by means of angular-momentum-vector coupling coefficients.[16] In view of the strong spin-orbit coupling in cesium, it is important to allow for the dependence of the bound-bound reduced matrix elements $\sigma(n'\,l-1\,j';nlj)$ on the quantum numbers j and j' of the valence electron. No such allowance has been made in the case of bound-free reduced matrix elements $\sigma(n\,l\pm1;\epsilon'l)$, since the spin-orbit interaction is greatest in the lower-lying levels of an atomic term series.

Estimates of $|\sigma(6s\tfrac{1}{2};npj')|$ and $|\sigma(npj';9dj)|$ for cesium with $n=6,\ldots,12$ are obtainable from the computed oscillator strengths of Stone.[17] These include corrections for spin-orbit coupling, indicating a particularly marked j' dependence of $\sigma(6s\tfrac{1}{2};npj')$ for $n=7,\ldots,12$. They compare favorably with estimates obtained by Coulomb-approximation methods,[18] from which relative signs of the matrix elements have been estimated. The bound-free matrix elements $\sigma(6s;\epsilon'p)$ and $\sigma(9d;\epsilon'p)$ have been obtained from extrapolated quantum defects and the tables of Peach,[19] and the integrals in Eqs. (A2) and (A3) evaluated graphically. Transition frequencies were obtained from appropriate spectroscopic tables.[20]

The final results are

$$\chi^{9D_{3/2}\leftarrow 6S_{1/2}}_{zzzz}(-\omega_\sigma;\omega_1,\omega_2,\omega_3)=(8.8\pm4)\times10^{-27}I_{1,2,3}\left(\frac{\frac{1}{2}\Gamma_{9D}}{\Omega_{9D_{3/2}}-\omega_1-\omega_2}\right), \tag{A9}$$

$$\chi^{9D_{5/2}\leftarrow 6S_{1/2}}_{zzzz}(-\omega_\sigma;\omega_1,\omega_2,\omega_3)=(15\pm9)\times10^{-27}I_{1,2,3}\left(\frac{\frac{1}{2}\Gamma_{9D}}{\Omega_{9D_{5/2}}-\omega_1-\omega_2}\right), \tag{A10}$$

in units of esu/atom. The numerical coefficient in (A9) may be identified with χ_0 of Eq. (15). In obtaining these results, the sums over A_n equations (A2) and (A3) are found to converge rapidly and the continuum contribution is small (~20% of the total). However, severe cancellations in the sums over B_n allow the contribution of $B(\epsilon')$ to be dominant. This contribution is enhanced approximately twofold by a resonance in $B(\epsilon')$ as $(I_{6S}+\epsilon')$ approaches ω_σ. The estimates of uncertainty in Eqs. (A9) and (A10) reflect these cancellations and the importance of continuum contributions.

It is of interest to note that the ratio of the numerical coefficients in Eqs. (A10) and (A9) is 1.7 ± 1.0, which differs only slightly from the ratio of 1.5 predicted for negligible spin-orbit coupling. This is because the major portions of the A- and B-type contributions arise, respectively, from $6p^2P$ and $\epsilon'p$ intermediate states, neither of which exhibits appreciable j dependence in its matrix elements. Measurements of the above ratio could provide an object for future study, with a laser tunable through both $9d\,^2D \leftarrow 6s\,^2S$ resonances.

Similar computational procedures have been used to calculate the polarizabilities $\alpha(\omega)$ and $\alpha(3\omega)$ which appear in Eq. (12). These are given by the formulas

$$\alpha(\omega')=\frac{e^2}{hc}\sum_n\left[\frac{1}{3}C_n\left(\frac{1}{2}\right)+\frac{2}{3}C_n\left(\frac{3}{2}\right)\right]+\frac{e^2}{hc}\int_0^\infty C(\epsilon')\,d\epsilon', \tag{A11}$$

$$C_n(j)=2\omega_{nP_j}(\omega^2_{nP_j}-\omega'^2)^{-1}\sigma^2(6s\tfrac{1}{2};npj), \tag{A12}$$

$$C(\epsilon')=2(I_{6S}+\epsilon')|(I_{6S}+\epsilon')^2-\omega'^2|^{-1}\sigma^2(6s;\epsilon'p)\,. \tag{A13}$$

For the frequencies relevant to the above experiments, namely, $\omega'=\omega$ and 3ω, we obtain polarizabilities of $(-115\pm5)\times10^{-24}$ and $(-4.3\pm0.5)\times10^{-24}$ esu/atom, respectively. The sums over discrete states converge rapidly, with all but the $n=6$ contributions negligible, and the continuum terms contribute −2.5 and −18% of the total, respectively.

*Research supported in part by the Air Force Office of Scientific Research under Grant No. 72-2302.

†Present address: Center for Laser Studies, University of Southern California, Los Angeles, Calif. 90007.

[1]K. M. Leung, Thesis (University of Michigan, 1972) (unpublished).

[2]B. J. Orr and J. F. Ward, Mol. Phys. 20, 513 (1971).

[3]J. F. Ward and G. H. C. New, Phys. Rev. 185, 57 (1969).

[4]R. Loudon, Proc. R. Soc. 82, 393 (1963). A. Javan and A. Szöke, Phys. Rev. A137, 536 (1935). P. N. Butcher, R. Loudon, and T. P. McLean, Proc. R. Soc. 85, 565

(1965). Y. R. Shen, Phys. Rev. A138, 1741 (1965). C. H. Henry and C. G. B. Garrett, J. Quantum Electron. 4, 353 (1968).
[5]R. W. Minck, R. W. Terhune, and C. C. Wang, Appl. Opt. 5, 1595 (1965).
[6]W. Kaiser and C. G. B. Garrett, Phys. Rev. Lett. 7, 229 (1961). J. A. Giordmaine and John A. Howe, Phys. Rev. Lett. 11, 207 (1963). J. L. Hall, D. A. Jennings, and R. M. McClintock, Phys. Rev. Lett. 11, 364 (1963).
[7]I. D. Abella, Phys. Rev. Lett. 9, 453 (1962).
[8]See, for example J. R. Izatt, R. C. Mitchell, and H. A. Daw, J. Appl. Phys. 37, 1558 (1960).
[9]R. E. Honig and D. A. Kramer, RCA Rev. 30, 285 (1969).
[10]P. Sitz and R. Yaris, J. Chem. Phys. 49, 3546 (1968).
[11]B. D. Fried and S. D. Conte, *The Plasma Dispersion Function* (Academic, New York, 1961).
[12]W. V. Houston, Phys. Rev. 54, 884 (1938); Chris Gregory, Phys. Rev. 61, 465 (1942).
[13]A. V. Smith (private communication).
[14]J. F. Young, G. C. Bjorklund, A. H. Kung, R. B. Miles, and S. E. Harris, Phys. Rev. Lett. 27, 1551 (1971).
[15]M. P. Bogaard, A. D. Buckingham, and B. J. Orr, Mol. Phys. 13, 533 (1967); M. P. Bogaard and B. J. Orr, Mol. Phys. 14, 557 (1968).
[16]A. R. Edmonds, *Angular Momentum in Quantum Mechanics* (Princeton U. P., Princeton, N. J., 1957); E. U. Condon and G. H. Shortley, *The Theory of Atomic Spectra* (Cambridge U. P., London, 1935).
[17]P. M. Stone, Phys. Rev. 127, 1151 (1962).
[18]D. R. Bates and A. Damgaard, Phil. Trans. R. Soc. Lond. A242, 101 (1949).
[19]G. Peach, Mem. R. Astron. Soc. 71, 13 (1967).
[20]C. E. Moore, *Atomic Energy Levels*, U. S. Dept. of Commerce, Natl. Bur. Std. (U. S. GPO, Washington, D. C., 1949).